DOI: 10.1002/ejic.201000115

Bis(3,5-dimethyl-4-vinylpyrazol-1-yl)acetic Acid: A New Heteroscorpionate Building Block for Copolymers that Mimic the 2-His-1-carboxylate Facial Triad

Gazi Türkoglu,[a] Cristina Pubill Ulldemolins,[a] Rainer Müller,[b] Eike Hübner,[a,c] Frank W. Heinemann,[a] Marion Wolf,[a] and Nicolai Burzlaff*[a]

Keywords: Ligand design / Copolymerisation / Manganese / Rhenium / Ruthenium / Tripodal ligands

The new *N,N,O* ligand bis(3,5-dimethyl-4-vinylpyrazol-1-yl)-acetic acid (Hbdmvpza) (**4**) suitable for copolymerisation was synthesised in a multi-step synthesis starting from bis(3,5-dimethylpyrazol-1-yl)methane (**1**). The κ^3-*N,N,O* facial coordination behaviour of **4** was verified by synthesis and characterisation of the tricarbonyl compounds [Mn(bdmvpza)$(CO)_3$] (**5**) and [Re(bdmvpza)$(CO)_3$] (**6**), the ruthenium bisphosphane complex [Ru(bdmvpza)Cl$(PPh_3)_2$] (**7**), as well as the complex [Cu(bdmvpza)$_2$] (**8**). Copolymerisation of **4** with methyl methacrylate (MMA) or ethylene glycol dimethacrylate (EGDMA) led to solid phases **P1a**, **P1b** and **P2** with different amounts of incorporated ligand **4**. Furthermore, a homopolymer **H1** of ligand **4** was successfully synthesised. Copolymer-bound manganese and rhenium tricarbonyl complexes **P1a-Mn**, **P1a-Re**, **P2-Mn** and **P2-Re** have been obtained by reaction of **P1a** and **P2** with the metal precursors [Mn$Br(CO)_5$] and [Re$Br(CO)_5$], respectively. The κ^3-*N,N,O* coordination of the manganese and rhenium centres was verified by IR spectroscopy and the amount of incorporated metal complex was determined by AAS or ICP-AES measurements. Treatment of the deprotonated copolymer **P1a** or **P2** with copper(II) or iron(II) led to polymers **P1a-Cu, P1a-Fe** and **P2-Fe**. A bathochromic shift in the UV spectrum of **P1a-Cu** compared to the absorption maximum of the homogeneous complex **8** by 64 nm indicates copper centres with one ligand moiety bound only. AAS analysis of **P1a-Fe** and **P2-Fe** show that up to 64 % of the ligand sites can be accessed with iron(II). Furthermore, two 2-oxocarboxylato complexes [Ru(bdmvpza)(BF)(PPh_3)] (**9**) (BF = benzoylformato) and [Ru(bdmvpza)(NOG)(PPh_3)] (**10**) (NOG = *N*-oxalylglycine) have been synthesised that mimic the shape of the active sites of 2-oxoglutarate dependent iron oxygenases. The successful copolymerisation of **9** and **10** with EGDMA was proven by UV spectroscopy.

Introduction

Transition metal complexes with bis(pyrazol-1-yl)acetic acids have proven to be good structural mimics for metalloenzymes.[1–5] Especially, the 2-His-1-carboxylate facial triad of 2-oxoglutarate (2-OG) dependent iron oxygenases (Figure 1) is well resembled by these ligands in which the pyrazole donors mimic the two histidines and the carboxylate emulates the aspartate. Unfortunately, due to their high binding affinity, sterically less-demanding bis(pyrazol-1-yl)-acetic acids such as bis(3,5-dimethylpyrazol-1-yl)acetic acids (Hbdmpza) form rather unreactive bisligand complexes which do not allow any further reactions with additional ligands or potential substrates.[1,2,6] Furthermore, especially in oxidation reactions, the formation of μ-oxo-bridged dinuclear complexes seems to be thermodynamically favoured. Solid phase fixation of *N,N,O* ligands via copolymerisation is a very elegant way to prevent the formation of 2:1 bisligand complexes.[7]

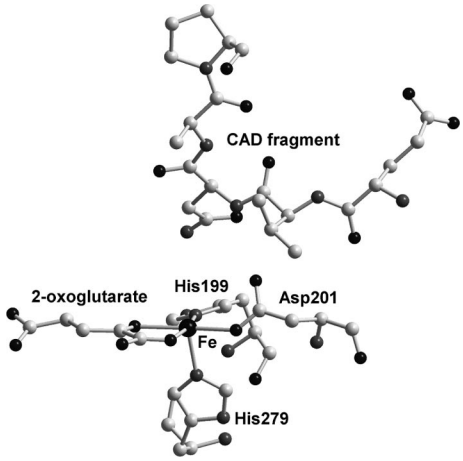

Figure 1. Active site of factor inhibiting HIF (FIH) with 2-OG and substrate fragment [PDB code: 1H2L].[8]

[a] Inorganic Chemistry, Department of Chemistry and Pharmacy & Interdisciplinary Centre for Molecular Materials (ICMM), University of Erlangen Nürnberg, Egerlandstraße 1, 91058 Erlangen, Germany
Fax: +49-9131-85-27387
E-mail: burzlaff@chemie.uni-erlangen.de
[b] Department of Chemistry, University of Konstanz, 78457 Konstanz, Germany
[c] Research Centre Jülich, Institute of Solid State Research, Neutron Scattering, 52425 Jülich, Germany

Besides, grafted ligands are of interest due to many advantages of supported catalysts such as an easy work up or a high recycling potential.[9–12] Examples for the application of grafted ligand systems for enzyme modeling and catalysis have been reported by Heinze et al.[13] and Severin et al.[14] Especially the imprinted polymer concept followed by Severin might allow access to artificial enzymes. Furthermore, Kunz et al.[15] described the utilisation of immobilised $[Tc(CO)_3]$ fragments for radiopharmaceutical purposes. Recently we presented the synthesis of a *N*,*N*,*O* ligand bearing a methacryloxy linker group.[7] This 2,2-bis(3,5-dimethylpyrazol-1-yl)-3-methacryloxypropionic acid (Hbdmpzmp) ligand was successfully copolymerised with either methyl methacrylate (MMA), a combination of MMA and ethylene glycol dimethylacrylate (EGDMA) or pure EGDMA yielding various copolymers as well as polymer-bound manganese and rhenium tricarbonyl complexes thereof. The shape of the active site of 2-OG dependent iron oxygenases can be mimicked by ruthenium(II) model complexes, as we reported some years ago with complexes such as [Ru(bdmpza)(2-OG)(PPh_3)] and [Ru(bdmpza)(O_2CC(=O)Ph)(PPh_3)].[5] Unfortunately, so far it was not possible to synthesise ruthenium(II) complexes with a κ^3-*N*,*N*,*O* coordinated bdmpzmp ligand suitable for copolymerisation. Recent studies suggest that a linker at the bridging carbon atom of a bis(3,5-dimethylpyrazol-1-yl)acetato (bdmpza) ligand does affect the remaining space at the κ^3-*N*,*N*,*O*-[Ru(bdmpzmp)] complex fragment and does prevent the formation of bulky model complexes such as [Ru(bdmpzmp)(2-OG)(PPh_3)] and [Ru(bdmpzmp)(O_2CC(O)Ph)(PPh_3)].[7,16,17] Here we report on a new approach toward such active-site-shaped and copolymersable ruthenium complexes with a new bis(3,5-dimethylpyrazol-1-yl)-acetate based ligand.

Results and Discussion

Ligand Design

In our former reports on bis(pyrazol-1-yl)acetic acids suitable for solid-phase fixation or copolymerisation, we described various ligands with linker groups at the bridging carbon atom of a bis(3,5-dimethylpyrazol-1-yl)acetic acid.[7,16] However, this type of modification can cause changes in the coordination behaviour as mentioned above. Furthermore, due to their flexibility, linker groups at the bridging carbon atom can cause chirality and thus enantiomers by dynamic interconversion.[7,16] Finally, the introduced linker group may occasionally compete with the carboxylate donor for coordination towards the metal center, as we reported recently for the bisligand copper complex [Cu(κ^2-*N*,*O*-bdmpzmp)$_2$] [bdmpzmp = 2,2-bis(3,5-dimethylpyrazol-1-yl)-3-methacryloxypropionate].[7] To avoid these problems, we chose a new approach for immobilisation of pyrazole-based ligands. Our aim was to generate bis(pyrazol-1-yl)acetic acids, in which the polymerisation-active linker is located directly at the pyrazole units. We assumed that bis(3,5-dimethyl-4-vinylpyrazole)acetic acid (Hbdmvpza) (**4**) with two vinyl moieties at positon 4 of the pyrazoles would be an appropriate candidate for this purpose.

The synthesis of this new 4-vinyl-substituted ligand **4** was achieved in three steps starting from easily accessible bis(3,5-dimethylpyrazole)methane[18] (**1**) (Scheme 1). In the first step, the bisaldehyde **2** was synthesised by a Vilsmeier reaction of **1** with phosphoryl chloride and dimethylformamide according to an procedure recently reported by Potapov, Khlebnikov and Ogorodnikov.[19] The bisaldehyde **2** then was converted into the vinyl-substituted product bis(3,5-dimethyl-4-vinylpyrazol-1-yl)methane (**3**) via a Wittig reaction. For this purpose, the ylide $Ph_3P{=}CH_2$ was generated by treating a suspension of methylenetriphenylphosphonium bromide in THF with KO*t*Bu. Reaction of the ylide with bisaldehyde **2** leads to the vinyl-substituted product **3** which was isolated by column chromatography in a good yield (Scheme 1).

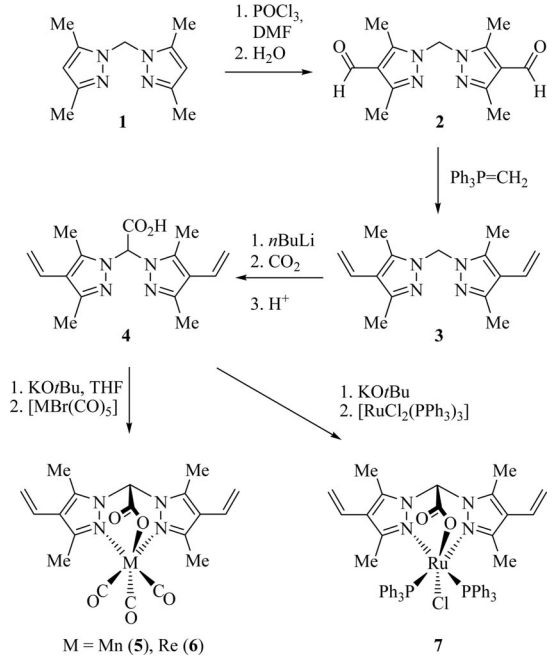

Scheme 1. Synthesis of the Hbdmvpza ligand **4** and its transition metal complexes [Mn(bdmvpza)$(CO)_3$] (**5**), [Re(bdmvpza)$(CO)_3$] (**6**) and [Ru(bdmvpza)Cl$(PPh_3)_2$] (**7**).

Successful formation of **3** was verified by NMR spectroscopy. An AMX resonance system[20] is observed for the vinyl group in the ^{1}H NMR spectrum of **3** with three sets of double doublet signals at δ = 5.13 and 5.28 ppm (the terminal protons of the vinyl groups) and δ = 6.46 (remaining =CH– proton) ppm. Furthermore, one set of signals for the pyrazolyl groups can be observed in the ^{1}H as well as in the ^{13}C NMR spectrum of **3**. This is consistent with C_S symmetry of the molecule in solution. The coupling constants of the vinyl groups have been determined to 1.4 Hz for the geminal ^2J coupling, 17.7 Hz for the $^3J(E)$ and 11.4 Hz for the $^3J(Z)$ coupling.

In the final step of the ligand synthesis, **3** is deprotonated with *n*-butyllithium at –80 °C and subsequently treated with CO_2. After aqueous work up ligand Hbdmvpza (**4**) can be isolated by extraction from the acidified (pH = 2) aqueous phase (Scheme 1). NMR spectroscopic data of the resulting ligand **4** are almost identical to those of ligand **3** except for additional ^{1}H and ^{13}C resonances of the introduced carboxylate group. A distinction of the carbon resonances was possible with a heteronuclear multiple quantum coherence (HMQC) experiment.

Synthesis of Transition Metal Complexes

In order to prove the tripodal κ^3-*N*,*N*,*O* coordination behaviour of the bdmvpza ligand **4**, several transition metal complexes have been synthesised and investigated. Tricarbonylmanganese and -rhenium complexes have been synthesised (Scheme 1) by deprotonation of ligand **4** with KO*t*Bu and subsequent reaction with the precursor compounds $[MnBr(CO)_5]$ and $[ReBr(CO)_5]$, respectively. The formation of the resulting complexes **5** and **6** can easily be monitored by IR spectroscopy due to a single A′ and two close A′′ and A′ carbonyl signals which are rather typical for facial tricarbonyl complexes with C_s symmetry. As shown in Table 1, the complexes **5** and **6** show almost identical IR absorption bands compared to tricarbonyl complexes bearing similar κ^3-*N*,*N*,*O*-bound bis(pyrazol-1-yl)-acetato ligands, which have been investigated in the past.[3,7]

Table 1. Selected IR signals (THF, wavenumbers, unit: cm^{-1}) of various complexes $[LMn(CO)_3]$ and $[LRe(CO)_3]$.

Ligand L	ν(CO) $[MnL(CO)_3]$	ν(CO) $[ReL(CO)_3]$
bdmvpza (anion of **4**)	2036, 1944, 1917	2026, 1921, 1898
bdmpza[3]	2036, 1942, 1915	2025, 1918, 1896
bpza[3]	2041, 1946, 1925	2029, 1924, 1904
bdmpzmp[7]	2034, 1940, 1913	2024, 1918, 1894

The successful formation of the tricarbonyl complexes **5** and **6** was also verified by NMR spectroscopy. In both cases, the ^{13}C NMR spectrum consists of a clear set of signals for the coordinated bdmvpza ligand. The resonance for the carboxylate group is found at δ = 165.5 ppm for the manganese complex **5** and at δ = 163.8 ppm in case of the rhenium complex **6**. Two ^{13}C signals for the carbonyl ligands can be observed for each compound (**6**: 223.1, 219.9 ppm, **7**: 196.0, 194.9 ppm). The ^{1}H NMR spectrum of the manganese compound **5** exhibits rather broad signals, due to fast relaxation caused by the quadrupole moment of ^{55}Mn. Thus, it was not possible to assign any couplings. On the other hand the ^{1}H NMR spectrum of the rhenium complex **6** presents sharp signals with an AMX resonance system as to expect.

Finally, a single-crystal X-ray structure of complex **5** doubtlessly reveals the correct κ^3-*N*,*N*,*O* coordination mode of the new 4-vinyl-substituted ligand **4** (Figure 2). Suitable crystals have been obtained by layering a dichloromethane solution of **5** with diethyl ether. The asymmetric unit of the cell contained two molecules of complex **5** of which one was slightly disordered. The distances and angles of the molecular structure agree well with those of other manganese tricarbonyl complexes bearing bis(pyrazol-1-yl)acetato ligands.[3,7] The distances *d*(Mn–C33) and *d*(Mn–C35) are slightly longer than *d*(Mn–C34) probably due to the π acceptor properties of the pyrazole donors and the resulting *trans* influence.

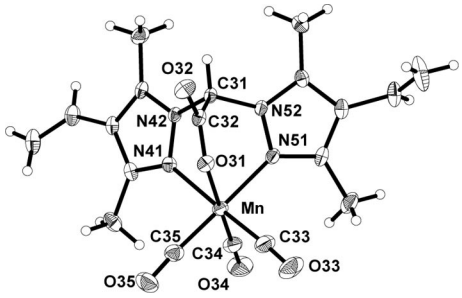

Figure 2. Molecular structure of $[Mn(bdmvpza)(CO)_3]$ (**5**); thermal ellipsoids are drawn at the 50% probability level. Depicted is only one of the two molecules in the asymmetric unit, which is not disordered. Selected bond lengths [Å] and angles [°]: *d*(Mn–N41) = 2.064(2), *d*(Mn–N51) = 2.066(2), *d*(Mn–O31) = 2.048(2), *d*(Mn–C33) = 1.812(3), *d*(Mn–C34) = 1.800(3), *d*(Mn–C35) = 1.813(3), ∠(N41,Mn,N51) = 86.12(9), ∠(N41,Mn,O31) = 84.27(8), ∠(N51,Mn,O31) = 85.48(8), ∠(C33,Mn,C34) = 91.55(15), ∠(C33,Mn,C35) = 86.10(15), ∠(C34,Mn,C35) = 91.22(15).

In our previous publications, we reported on *N*,*N*,*O* ligands which are suitable for copolymerisation and immobilisation, where either a linker functionality or a polymerisation active unit was introduced at the bridging carbon atom of bis(pyrazol-1-yl)acetic acid.[7,16] Unfortunately due to competitive and steric effects, we never were able to synthesise facial coordinated ruthenium complexes with those ligands, as mentioned above. On a parallel project, we are currently studying the influence of substituents at this bridging position and the results hereof will be presented soon.[17] In contrast to the ligands described above, our new ligand **4** should be able to bind ruthenium facially without any interference of the vinyl groups with the ruthenium centre. Indeed, the bisphosphane ruthenium complex $[Ru(bdmvpza)Cl(PPh_3)_3]$ (**7**) was successfully synthesised by deprotonation of ligand **4** followed by a reaction with the precursor $[RuCl_2(PPh_3)_3]$ (Scheme 1). A single signal in the ^{31}P NMR spectrum of **7** (δ = 35.1 ppm) as well as one set of signals for the pyrazolyl groups in the ^{1}H and ^{13}C NMR spectra indicate a symmetric geometry for complex **7**, with the remaining chlorido ligand in *trans* position to the carboxylate functionality. Moreover, the successful formation of bisphosphane complex **7** was verified by elemental analysis and the asymmetric carboxylate vibration in the IR spectrum at $\tilde{\nu}$ = 1669 cm^{-1}, which is in good agreement with the very similar bisphosphane complex $[Ru(bdmpza)Cl(PPh_3)_2]$.[21]

Homo- and Copolymerisation of 3 and 4

The heteroscorpionate *N*,*N*,*O* ligand **4** as well as the neutral *N*,*N* chelating ligand **3** have been investigated regarding their properties as potential polymer building blocks. It is noteworthy, that ligands **3** and **4** as well as their transition metal complexes can act as crosslinking agents due to two polymerisation active vinyl groups. This is in contrast to the ligand systems we reported on previously, where the synthesis of highly crosslinked networks of polymer-ligand hybrid material was only possible by copolymerisation in presence of additional monomers such as EGDMA. Furthermore, **3** or **4** copolymerise with methyl methacrylate (MMA) or ethylene glycol dimethacrylate (EGDMA) as co-monomer (see Scheme 2 and Figure 3). Ligand **4** does also polymerise to a homopolymer **H1**, by reacting **4** by oneself with the radical initiator azobis(isobutyronitrile) (AIBN). The amount of incorporation can be determined by the %N value of the elemental analysis of the resulting polymer. A very high amount of 3.05 mmol ligand per gram polymer was determined, as to expect for such a homopolymer (Table 2).

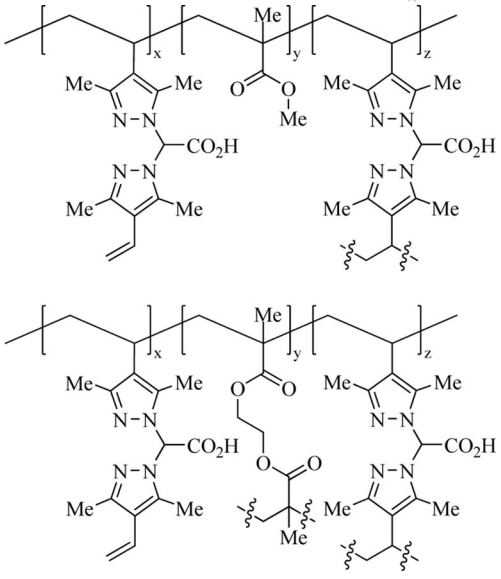

Figure 3. Possible formular structure of copolymers of **4** with MMA (top) and/or EGDMA (bottom). Due to the free radical polymerisation, atactic arrangement has to be assumed.

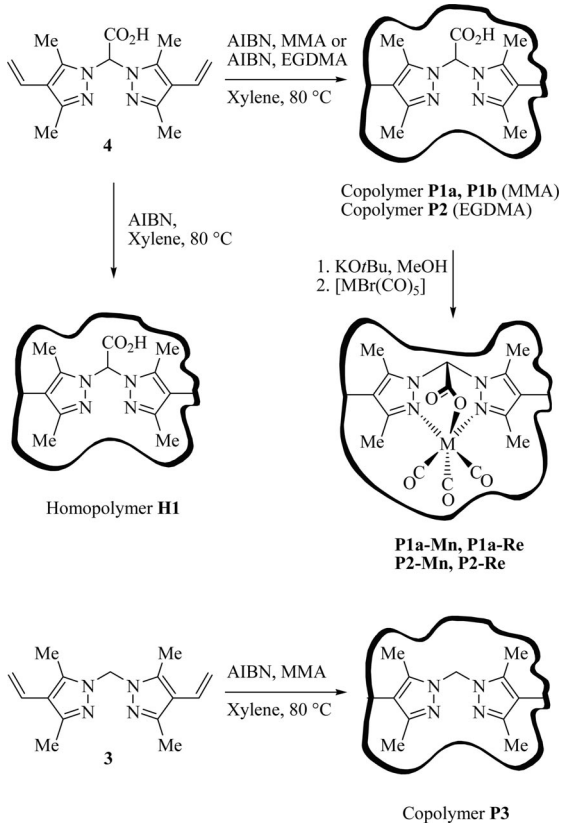

Scheme 2. Polymerisation of **3** and **4** and incorporation of Mn and Re as tricarbonyl complexes into the copolymers **P1a** and **P2**.

In case of the copolymerisation of ligand **4** with MMA, two different products can be isolated. A white precipitate **P1a** is formed during the reaction in xylene and was separated by filtration. Furthermore, when pouring the remaining filtrate into methanol, a second polymer **P1b** starts to precipitate. This observation might be explained by a smaller reactivity ratio of MMA compared to the crosslinking ligand **4**. We assume that highly reactive crosslinking ligand molecules **4** will tend to react preferentially with each other at the beginning of the polymerisation, forming a star like polymer[22] with a highly crosslinked core. As the reaction proceeds, the ratio of MMA and crosslinking ligand **4** lies in a range where a high molecular weight but soluble polymer **P1b** is formed. To corroborate this theory, the incorporation rate of both polymers **P1a** and **P1b** was determined after washing with appropriate solvents and drying. While in case of **P1a** 0.746 mmol ligand molecules per gram polymer have been incorporated at a ligand/monomer ratio of 0.302 mmol/g. A lower incorporation rate (0.304 mmol/g) is observed for **P1b** as expected.

Table 2. Incorporation of bdmvpzm (**3**) and Hbdmvpza (**4**) in polymers.

Polymer	Added monomer	Ligand/monomer [mmol/g][a]	Nitrogen content [%]	Ligand/polymer [mmol/g][b]	Yield [%][c]
P1a	MMA	0.302	4.14	0.746	31
P1b	MMA	0.302	1.70	0.304	12
P2	EGDMA	0.302	2.06	0.371	77
P3	MMA	0.354	2.91	0.520	68
H1	none	3.33	17.1	3.05	71

[a] Ratio related to composition in feed. [b] Ratio related to composition in final polymer. [c] Weight percent related to total weight of monomers in feed.

Reaction of **4** with EGDMA results in a highly crosslinked, intractable polymer **P2** which precipitates from the initially clear solution during the reaction. No further polymer can be isolated from the remaining filtrate. For **P2**, an incorporation rate of 0.371 mmol ligand per gram polymer was determined at the same ligand/monomer ratio of 0.302 mmol/g. Once again, this incorporation rate is significantly higher than the results we obtained previously for the Hbdmpzmp ligand.[7] In a third experiment, the neutral *N*,*N* chelating ligand **3** was copolymerised with MMA. In this case, the rather apolar copolymer **P3** stays in solution during the reaction. The precipitation of **P3** can be enforced by slowly pouring the reaction mixture into a polar solvent such as methanol. An incorporation of 0.520 mmol ligand per gram polymer was determined for **P3**.

The soluble polymers **P1b** and **P3** have been analysed by size exclusion chromatography (SEC). But as expected for crosslinked polymers, a very broad molecular mass distribution reaching from 5×10^3 to 1×10^7 g/mol was observed in both cases. Thus, only careful statements concerning the molecular structure of the polymers can be made. This is especially true, since the standards applied in SEC measurements regard to non-crosslinked polymers. The maximum of the molecular mass distribution of **P1b** and **P3** was found around 2×10^4 g/mol and 3×10^4 g/mol, respectively. But it remains unclear whether these values can be assigned to long single chains or to several shorter chains crosslinked together by ligands **3** or **4**. It is very likely that the broad mass distribution is due to random crosslinking of these units. An SEC analysis of highly crosslinked polymers **P1a** and **P2** and the homopolymer **H1** was not possible, due to their insolubility.

Manganese- and Rhenium-Containing Copolymers

In order to prove the κ^3 binding mode of the polymer embedded ligand fragments, we synthesised the immobilised manganese and rhenium tricarbonyl complexes by deprotonating **P1a** and **P2** with potassium *tert*-butoxide and subsequent reaction with $[MnBr(CO)_5]$ or $[ReBr(CO)_5]$ (Scheme 2). The highly crosslinked polymers stay insoluble during the reaction. For each metal-containing polymer **P1a-Mn**, **P1a-Re**, **P2-Mn**, and **P2-Re**, IR absorptions characteristic for facial tricarbonyl complexes (single A′ and two close A′′ and A′) are observed (**P1a-Mn**: 2038, 1947, 1918 cm^{-1}, **P1a-Re**: 2028, 1923, 1898 cm^{-1}, **P2-Mn**: 2041, 1949, 1924 cm^{-1}, and **P2-Re**: 2031, 1927, 1908 cm^{-1}) (Figure 4).

These signals agree well with those of the homogeneous tricarbonyl complexes **5** and **6** and prove the successful formation of the κ^3-*N*,*N*,*O* coordinated manganese and rhenium tricarbonyl moieties. In a control experiment, the reaction product of PMMA (polymethylmethacrylate) with $[ReBr(CO)_5]$ showed no carbonyl signals in the IR spectrum (Figure 4, g). In order to investigate the occupancy of the copolymerised ligand sites, the metal content was determined by AAS for the manganese-containing polymers

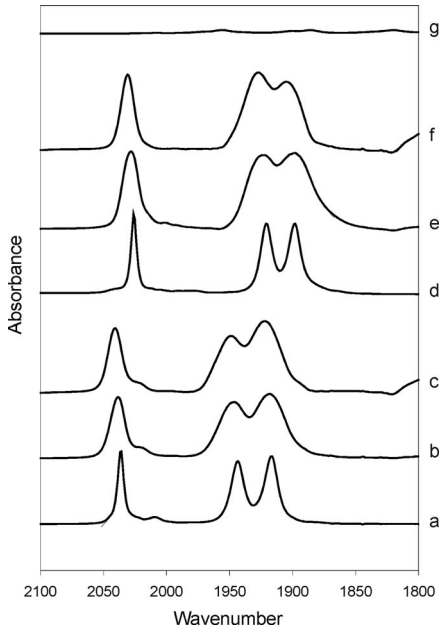

Figure 4. IR spectra of (a) $[Mn(bdmvpza)(CO)_3]$ (**5**) (THF), (b) the incorporated manganese complex **P1a-Mn** (nujol), (c) the incorporated manganese complex **P2-Mn** (nujol), (d) $[Re(bdmvpza)(CO)_3]$ (**6**) (THF), (e) the incorporated rhenium complex **P1a-Re** (nujol), (f) the incorporated rhenium complex **P2-Re** (nujol) and (g) a control experiment with PMMA and $[ReBr(CO)_5]$ (nujol).

P1a-Mn and **P2-Mn** and by ICP-AES measurements for the rhenium-containing polymers **P1a-Re** and **P2-Re** (Table 3).

Table 3. Metal content of the polymers **P1a-Mn/Re** and **P2-Mn/Re**.

Polymer	Metal/polymer [mg/g]	Metal/polymer [mmol/g]	Occupied ligand sites [%]
P1a-Mn	25.8[a]	0.470	63
P1a-Re	57.9[b]	0.311	42
P2-Mn	8.10[a]	0.148	40
P2-Re	7.11[b]	0.038	10

[a] Determined by AAS. [b] Determined by ICP-AES.

In case of the MMA crosslinked copolymer **P1a**, the amount of metal was found to be 25.8 mg of Manganese per gram of polymer **P1a-Mn** and 57.9 mg of Rhenium per gram of polymer **P1a-Re** respectively. This equals an occupancy of 63% (**P1a-Mn**) and 42% (**P1a-Re**) of the existing *N*,*N*,*O* binding sites of copolymer **P1a**. For the EGDMA crosslinked copolymer **P2** the occupancies are lower than those of **P1a**. In **P2-Mn** after all 40% of the ligand sites are bound to manganese centres, and in **P2-Re** 10% of the binding sites are occupied by rhenium atoms. The lower incorporation may be explained by a more restricted access to the ligand sites due to the additional crosslinking by EGDMA.

Copper- and Iron-Containing Complexes and Copolymers

Sterically less demanding tripod ligands such as bis(pyrazol-1-yl)acetic acid or bis(3,5-dimethylpyrazol-1-yl)-

acetic acid tend to form undesired 2:1 bisligand complexes with many transition metals.[1,2,6,7] These bisligand complexes are not suitable for further studies on enzyme models since they are coordinatively saturated and unreactive towards possible substrate molecules. As our recent report on the methacryloxy substituted ligand Hbdmpzmp has shown, a heterogeneous reaction of copper(II) with a highly crosslinked solid phase allows to control the copper coordination geometry and to favour 1:1 metal to ligand moieties instead of bisligand moieties.[7] To investigate whether the vinyl-substituted ligand Hbdmvpza (**4**) facilitates also the control of coordination geometries in crosslinked polymers, we also focused on embedded copper(II) complexes. For comparison reasons the homogeneous, turquoise 2:1 bisligand complex [Cu(bdmvpza)$_2$] (**8**) was synthesised by reacting ligand **4** in acetonitrile with copper(II)acetate (Scheme 3).

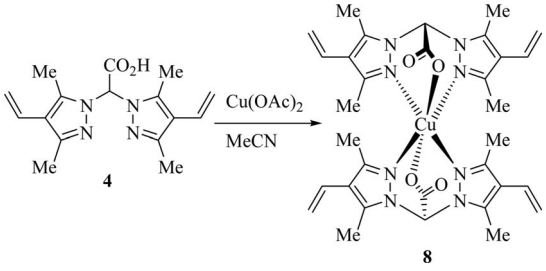

Scheme 3. Synthesis of the 2:1 bisligand complex [Cu(bdmvpza)$_2$] (**8**).

The IR spectrum of **8** exhibits a strong asymmetric carboxylate vibration at $\tilde{\nu}$ = 1664 cm^{-1}. An additional band at $\tilde{\nu}$ = 1636 cm^{-1} was assigned to the vinyl-C=C vibration. The result of a single-crystal X-ray structure analysis confirms the successful formation of the bisligand complex [Cu(bdmvpza)$_2$] (**8**) and verifies the κ^3-*N*,*N*,*O* coordination (Figure 5). In the molecular structure of **8** the Cu^{II} centre is placed on a special position, with half a molecule of [Cu(bdmvpza)$_2$] in the asymmetric unit. Complex **8** represents a Jahn–Teller distorted octahedral geometry. The basal plane is build up by the nitrogen atoms N11 and N11a [*d*(N11a–Cu) = 2.141(3) Å] and the two oxygen atoms O1a and O1b [*d*(O1a–Cu) = 1.951(2) Å] of the carboxylate donors. The nitrogen atoms N21a and N21b form the Jahn–Teller axis with *d*(N21a–Cu) = 2.278(3) Å. These results are in very good agreement to those, reported by Reedijk et al. for the complex [Cu(bdmpza)$_2$].[6]

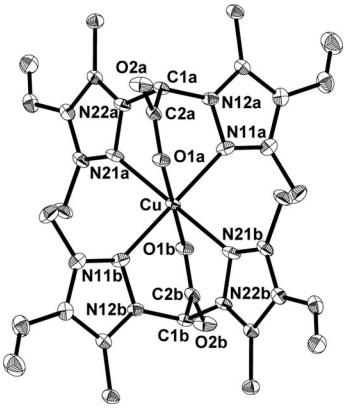

Figure 5. Molecular structure of [Cu(bdmvpza)$_2$] (**8**); thermal ellipsoids are drawn at the 50% probability level. Hydrogen atoms and disordered solvent molecule have been omitted for clarity. Selected bond lengths [Å] and angles [°]: *d*(Cu–N11a) = 2.141(3), *d*(Cu–N21a) = 2.278(3), *d*(Cu-O1a) = 1.951(2), ∠(N11a,Cu,N21a) = 84.82(9), ∠(N11a,Cu,O1a) = 85.76(9), ∠(N21a,Cu,O1a) = 85.14(9).

In order to generate a copolymer with 1:1 Cu/ligand moieties, polymer **P1a** was deprotonated with potassium *tert*-butoxide in methanol. Addition of $CuCl_2$ to this suspension caused an instant colour change of the polymer to green (Scheme 4). **P1a-Cu** was isolated as a green powder after filtration and washing with methanol.

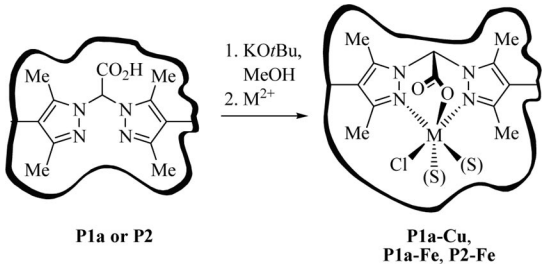

Scheme 4. Incorporation of copper and iron into copolymers **P1a** and **P2**.

To prove the successful incorporation of copper into copolymer **P1a** and to further investigate the binding mode of the copper centres, UV/Vis spectra of copolymer **P1a-Cu** and the homogeneous 2:1 bisligand complex [Cu(bdmvpza)$_2$] (**8**) have been compared with each other (Figure 6). For this purpose, a thin polymer pellet of **P1a-Cu** was prepared by a hydraulic press. A drop of mineral oil

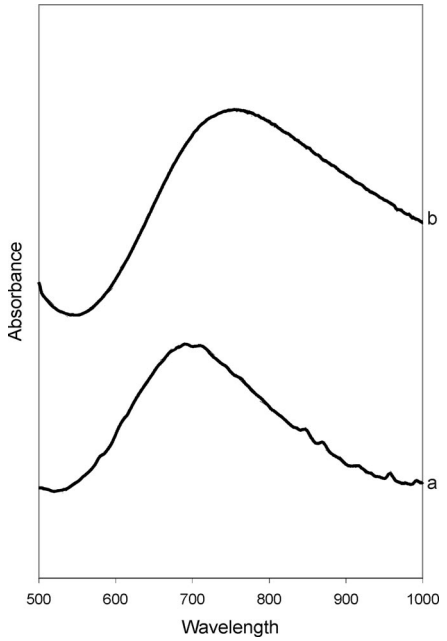

Figure 6. UV/Vis spectra of (a) [Cu(bdmvpza)$_2$] (**7**) in methanol and (b) **P1a-Cu** (polymer pellet, nujol).

(spectroscopy grade) was used to make the pellet transparent. Prior to UV/Vis measurement, a baseline was collected using a PMMA pellet of the same thickness which was prepared analogously. For the copolymer **P1a-Cu** a bathochromic shift of the absorption maximum by 64 nm is observed. This agrees well with a similar bathochromic shift we observed for copper-containing copolymers of the methacryloxy-substituted ligand Hbdmpzmp.[7] Due to the bathochromic shift the formation of one-sided κ^3-*N*,*N*,*O*-bound copper centres and 1:1 complex moieties can be assumed, although so far other coordination modes such as κ^2-*N*,*O* can not be excluded entirely.

To investigate the incorporation of ferrous iron **P1a** or **P2** were deprotonated with KO*t*Bu and treated with a slight excess of Fe^{II} in a similar procedure. The resulting pale greenish, air sensitive polymers were washed with degassed methanol and dried in vacuo prior to determination of the metal content by AAS measurement. In order to prove reproducibility with different metal sources, we treated deprotonated **P1a** with $FeCl_2$ or $FeSO_4$ in two separate experiments. The determined amounts of iron were almost identical for both cases (0.491 mmol g^{-1} and 0.448 mmol g^{-1}). This means that up to 64% of the *N*,*N*,*O* binding sites in polymer **P1a** can be occupied by ferrous centres. It is noteworthy that a similar high incorporation rate was achieved in case of the EGDMA crosslinked polymer **P2-Fe** (0.165 mmol g^{-1}). Surprisingly, nearly 60% of the *N*,*N*,*O* sites in **P2-Fe** were occupied by iron(II) ions, although a restricted access to these sites can be assumed due to higher crosslinking.

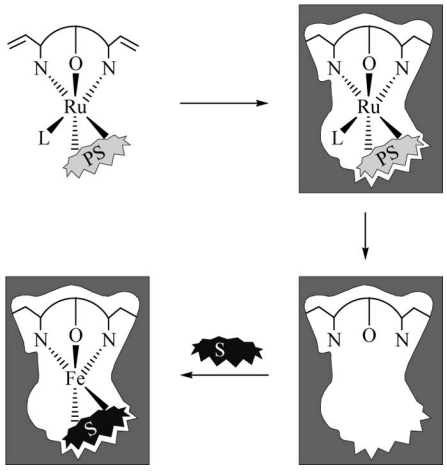

Scheme 5. Concept towards an artificial enzyme by applying imprinted polymer techniques (PS = pseudo substrate or substrate analogue bound to a dummy complex, S = natural substrate).

Polymerisation of Ruthenium Template Complexes

One aim of our research is the synthesis and investigation of model complexes for mononuclear iron oxygenases that exhibit a so called 2-his-1-carboxylate facial triad as metal binding motif. Unfortunately the spectroscopic characterisation of iron(II) complexes with tripod *N*,*N*,*O* ligands is difficult, due to their paramagnetic properties and the fact that they are easily oxidised. However, analogous ruthenium(II) complexes are diamagnetic and can thus be easily characterised by NMR spectroscopy. Examples of hemilabile carboxylato and 2-oxocarboxylato ruthenium complexes bearing the Hbdmpza ligand as model complexes for 2-oxoglutarate (2-OG) dependent iron enzymes have been published by our group before.[5,23] With our new ligand Hbdmvpza (**4**) which is suitable for copolymerisation but also capable of binding ruthenium with the κ^3-*N*,*N*,*O* motif, a door to imprinted polymer techniques might be opened (Scheme 5).

The concept behind imprinted polymers is to synthesise a dummy complex e.g. with ruthenium bearing a pseudo substrate or substrate analogue **PS** similar in shape to the real (co)substrate **S**.[14] Copolymerisation of this template molecule with EGDMA/MMA followed by extraction of the dummy moiety might result in cavities complementary in shape to the active site of the enzyme. Thus, ferrous iron and the real substrate **S** can be recognized in a high selectivity and an artificial enzyme might be generated. On our route towards this imprinting concept, we succeeded to synthesise two new 2-oxocarboxylato complexes. The benzoylformato (BF) complex [Ru(bdmvpza)(BF)(PPh_3)] (**9**) was achieved by a reaction of **7** with thallous acetate in presence of benzoylformic acid (Scheme 6). During this one pot synthesis, the $\kappa^2O^1,O^{1'}$-carboxylato complex [Ru(bdmvpza)(O_2CMe)(PPh_3)] is formed in situ. As the reaction proceeds, the acetato ligand is exchanged by the BF ligand and complex **9** starts to precipitate out of the CH_2Cl_2 solution.

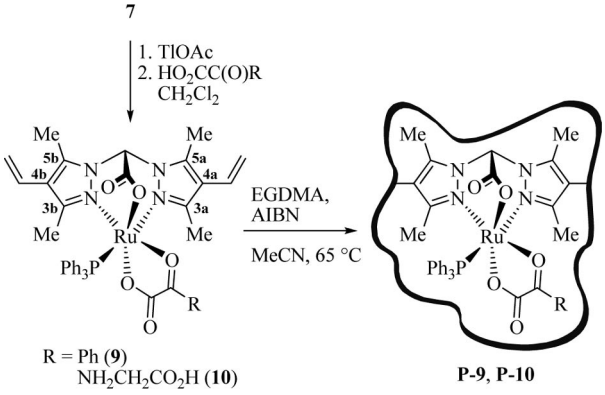

Scheme 6. Synthesis of 2-oxocarboylato complexes [Ru(bdmvpza)(BF)(PPh_3)] (**9**) and [Ru(bdmvpza)(NOG)(PPh_3)] (**10**) and copolymerisation with EGDMA (**P-9**, **P-10**).

In a similar procedure, [Ru(bdmvpza)(NOG)(PPh_3)] (**10**) was prepared by using *N*-oxalylglycine (NOG). Since NOG is isostructural to 2-oxoglutaric acid (2-OG) and thus a co-substrate analogue and inhibitor, complex **10** can be considered as a model complex for a 2-OG-dependent iron(II) enzyme inhibited by NOG and is well suited as a "dummy" complex for an imprinting attempt.

Successful formation of complexes **9** and **10** was verified by elemental analysis and NMR spectroscopy. The ^{31}P spectra of **9** and **10** exhibit a single signal for the remaining

PPh_3 ligand, thus proving the loss of the other one. Furthermore, two sets of signals assigned to the pyrazolyl groups are detected in the ^1H and ^{13}C spectra. This is in accordance to the chiral geometry of these complexes **9** and **10**. The UV spectrum of **9** exibits an intense maximum at λ = 555 nm corresponding to the deep purple colour of this compound whereas for the orange coloured complex **10** an absorption at λ = 300 nm can be observed. An X-ray structure analysis of **10** reveals the successful coordination of the NOG inhibitor (Figure 7). The molecular structure exhibits a *trans* geometry regarding both carboxylate donors. Contrary to this observation, usually the 2-oxo group is *trans* to the iron-binding aspartate in the active sites of most 2-oxoglutarate-dependent enzymes (Figure 1). In our previous investigations with 2-oxocarboxylato complexes we already reported on the formation of two structural isomers in case of prolonged reaction times.[5] Thus, currently we focus on the synthesis and isolation of this second isomer of **10** which might exhibit a correctly bound NOG inhibitor just by applying shorter reaction times. A synthesis of the analogous bdmpza complex [Ru(bdmpza)(NOG)$(PPh)_3$] (**11**) already resulted in the correct geometry (Figure 8).

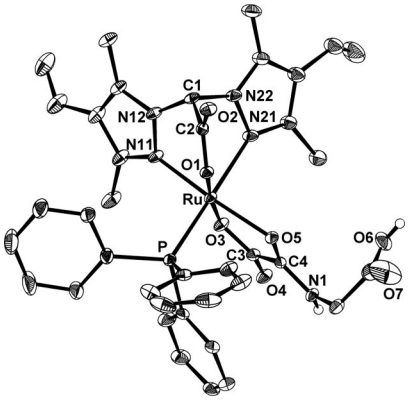

Figure 7. Molecular structure of [Ru(bdmvpza)(NOG)(PPh_3)] (**10**); thermal ellipsoids are drawn at the 50% probability level. Only one out of two molecules in the asymmetric unit is depicted and hydrogen atoms as well as the disordered solvent molecule have been omitted for clarity. Selected bond lengths [Å] and angles [°]: Ru–N11 2.037(3), Ru–N21 2.180(3), Ru–O1 2.086(2), Ru–O3 2.104(2), Ru–O5 2.134(2), Ru–P 2.2767(9), O3–C3 1.272(4), O4–C3 1.237(4), C3–C4 1.531(4), C4–N1 1.314(4), O5–C4 1.258(3); N11–Ru–N21 83.37(11), O1–Ru–N11 88.18(9), O1–Ru–N21 86.18(9), O1–Ru–P 86.39(6), O1–Ru–O3 174.20(8), O1–Ru–O5 96.68(8), N21–Ru–P 172.44(7), N11–Ru–O3 97.02(9).

Finally, complexes **9** and **10**, have been copolymerised with EGDMA in the presence of radical initiator AIBN. Acetonitrile was used as porogene solvent during these reactions to guarantee accessibility of the complex sites. UV spectra of the copolymers **P-9** and **P-10** have been compared to the free complexes [Ru(bdmvpza)(BF)(PPh_3)] (**9**) and [Ru(bdmvpza)(NOG)(PPh_3)] (**10**), respectively (Figure 9). In case of **P-9** and **P-10**, the UV/Vis spectra were recorded using nujol mulls of the finely ground polymer samples. An analogously prepared mull of PEGDMA in nujol was used for baseline collection.

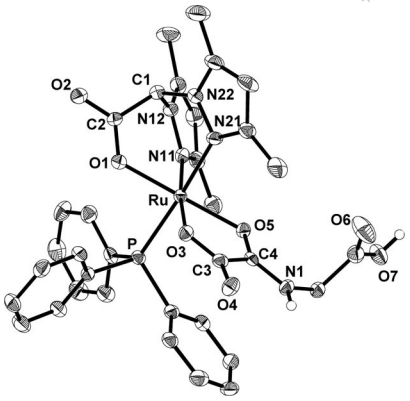

Figure 8. Molecular structure of [Ru(bdmvpza)(NOG)(PPh_3)] (**11**); thermal ellipsoids are drawn at the 50% probability level. Most hydrogen atoms as well as the solvent molecule have been omitted for clarity. Selected bond lengths [Å] and angles [°]: Ru–N11 2.062(4), Ru–N21 2.163(4), Ru–O1 2.088(3), Ru–O3 2.108(3), Ru–O5 2.107(3), Ru–P 2.2943(16), O3–C3 1.272(6), O4–C3 1.242(6), C3–C4 1.529(7), C4–N1 1.306(6), O5–C4 1.272(5); N11–Ru–N21 84.35(16), O1–Ru–N11 86.56(15), O1–Ru–N21 85.93(15), O1–Ru–P 89.60(10), O1–Ru–O3 96.92(14), O1–Ru–O5 175.65(13), N21–Ru–P 173.29(12), N11–Ru–O3 172.58(14).

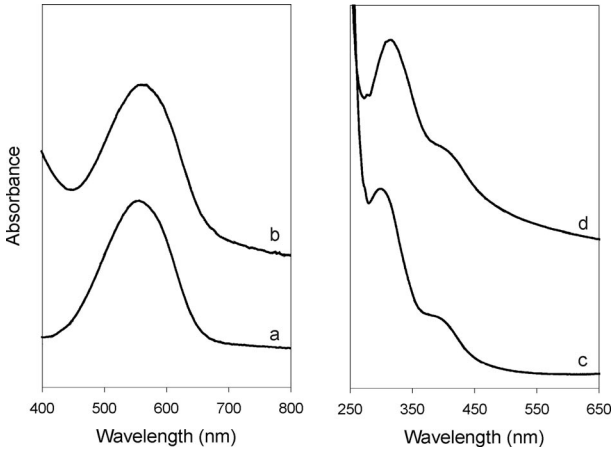

Figure 9. UV/Vis spectra of (a) [Ru(bdmvpza)(BF)(PPh_3)] (**9**) (in MeOH), (b) polymer **P-9** (nujol mull), (c) [Ru(bdmvpza)-(NOG)(PPh_3)] (**10**) (in DMF), (d) polymer **P-10** (nujol mull).

For both polymers **P-9** and **P-10** almost identical absorption maxima compared to the homogeneous complexes are observed, proving the successful incorporation of the complexes into the polymers. In our ongoing and long term project to develop functional model complexes for 2-OG dependent iron oxygenases, polymer embedded model complexes seem to be a promising approach to such artificial enzymes. Imprinted polymers assembled around ruthenium dummy complexes such as **P-9** and **P1-0** might in the future allow access to ferrous-containing artificial polymers once the inert low spin ruthenium(II) is replaced by a catalytically active ferrous high spin centre. Experiments in this regard to replace the [Ru(NOG)PPh_3] fragment are in progress.

Conclusion and Outlook

The new heteroscorpionate ligand bis(3,5-dimethyl-4-vinylpyrazol-1-yl)acetic acid (Hbdmvpza) (**4**) is synthesised by a Wittig reaction starting from bis(3,5-dimethyl-4-formylpyrazol-1-yl)methane (**2**) followed by a deprotonation and subsequent carboxylation with CO_2. Tricarbonyl complexes [Mn(bdmvpza)$(CO)_3$] (**5**) and [Re(bdmvpza)$(CO)_3$] (**6**) as well as the bisligand complex [Cu(bdmvpza)$_2$] (**8**) prove the κ^3-*N*,*N*,*O* coordination mode of ligand **4**. Furthermore, ligand **4** is also able to bind ruthenium(II) in a *fac*-κ^3-*N*,*N*,*O* mode. This was proven by synthesis of a bisphosphane complex [Ru(bdmvpza)Cl$(PPh_3)_2$] (**7**). Copolymerisation of ligand **4** with methyl methacrylate (MMA) or ethylene glycol dimethacrylate (EGDMA) yields copolymers **P1a** and **P2** with high amounts of embedded ligand **4**. Furthermore ligand **4** can also form a unique homopolymer **H1**. The ability of these copolymers to provide *N*,*N*,*O* binding sites is verified by a successful incorporation of *fac*-[Mn$(CO)_3$] and *fac*-[Re$(CO)_3$] fragments. This was monitored by IR spectroscopy. A heterogeneous reaction of the MMA copolymer of ligand **4** with $CuCl_2$ yields a solid phase which reveals a bathochromic shift by 64 nm compared to the UV/Vis spectrum of [Cu(bdmvpza)$_2$] (**7**). This implies, that copper(II) centers embedded in this copolymer are mainly coordinated by one ligand moiety. Successful incorporation of iron(II) was accomplished and proven by AAS measurements. Up to 64% of the ligand sites in the MMA-copolymer of ligand **4** can be occupied by ferrous iron centres. The ability of polymerization active Hbdmvpza (**4**) to bind ruthenium with the κ^3-*N*,*N*,*O* motif, opens a door to imprinted polymer techniques (Scheme 5). Two well suited "dummy" complexes have been synthesized and characterized, namely the 2-oxocarboxylato complex [Ru(bdmvpza)(BF)(PPh_3)] (**9**) and the inhibitor complex [Ru(bdmvpza)(NOG)(PPh_3)] (**10**). Polymerisation of **9** and **10** with EGDMA while maintaining the *fac*-κ^3-*N*,*N*,*O* coordination was successful. Thus, the generation of imprinted polymers with the new ligand **4** in upcoming studies seems quite promising.

Experimental Section

General Remarks: All operations were carried out under an inert gas atmosphere by applying conventional Schlenk techniques. The yields refer to analytically pure substances. IR spectra were recorded with an Excalibur FTS-3500 FTIR in CaF_2 cuvets (0.2 mm), KBr matrix or Nujol. ^{1}H, ^{13}C, ^{31}P and 2D NMR spectra were measured with a Bruker AC 250 and a Bruker DPX300 Avance instrument. The δ values are given relative to tetramethylsilane (^{1}H), the deuterated solvent (^{13}C) or, to PPh_3 (δ = –4.72 ppm) as internal standard (^{31}P). Mass spectra were recorded with a Finnigan MAT 312 and a Jeol JMS-700 instrument by using either FD or FAB technique with 3-nitrobenyzl alcohol as matrix. UV/Vis spectra were recorded on a Varian Cary-50 spectrometer using a quartz cuvette (d = 1 cm). In case of **P1a-Cu** a thin polymer pellet was prepared for UV/Vis measurements by applying a Perkin–Elmer hydraulic press mineral oil (Acros Organics, spectroscopy grade) to make the pellet transparent (baseline: PMMA pellet of the same thickness). UV/Vis spectra of **P-9** and **P-10** were recorded using nujol mulls of the finely ground polymer samples (baseline: PEGDMA mull in nujol). Elementary analyses were determined with a Euro EA 3000 (Euro Vector) and EA 1108 (Carlo Erba) instrument ($\sigma = \pm 1$% of the measured content). AAS: Perkin–Elmer 5100 F-AAS with AS-90 sample automation, acetylene/air flame (flow rates acetylene/air [L min^{-1}]: Cu 0.9/9.9, Mn 2.0/8.1, Fe 2.0/9.2; wavelength/spectral band width [nm]: Cu 324.8/0.7, Mn 279.8/0.7 nm, Fe 248.8/0.2; method of calibration: standard addition). A Spectro Analytical Instruments Spectroflame instrument was used for ICP-AES measurements [radial plasma view, argon gas flow rates: 12.8 L min^{-1} (coolant), 0.7 L min^{-1} (auxiliary), 0.5 L min^{-1} (carrier), wavelength Re/detection mode: 227.525 nm/sequential and 221.426 nm/sequential, method of calibration: standard addition]. A modified Siemens P4 diffractometer and a Bruker-Nonius Kappa-CCD were used for X-ray structure determination. SEC experiments were carried out using a PL-GPC 220 instrument with three Polypore (Polymer Laboratories) 5 micron colums at 30 °C (Solvent: THF/*N*,*N*-dimethylacetamide 85:15 v/v; flow rate: 1 mL/min, calibration: conventional polystyrene calibration). Prior to use MMA and EGDMA were washed with diluted NaOH, dried with Na_2SO_4, distilled and stored at –30 °C. All other solvents were used as purchased without further purification and degassed prior to use. Bis(3,5-dimethylpyrazol-1-yl)-methane,[18] bis(3,5-dimethyl-4-formylpyrazol-1-yl)methane,[19] [Ru(bdmpza)Cl$(PPh_3)_2$],[21] [Ru(bdmpza)$(O_2CCH_3)(PPh_3)$],[5,23] [Mn$Br(CO)_5$],[24] [Re$Br(CO)_5$],[24] [Ru$Cl_2(PPh_3)_3$],[25] and *N*-oxalylglycine hydrate[26] were synthesised according to literature.

Synthesis of Bis(3,5-dimethyl-4-vinylpyrazol-1-yl)methane (3): To a suspension of methyltriphenylphosphonium bromide (8.23 g, 23.1 mmol) in dry THF is added potassium *tert*-butoxide (2.41 g, 21.3 mmol). After stirring at ambient temperature for 1 h, bis(3,5-dimethyl-4-formylpyrazol-1-yl)methane (**2**) (2.00 g, 7.68 mmol) is added in small portions and the mixture is stirred overnight. Solids were filtered off and the solvent removed under reduced pressure. The crude product can be purified by column chromatography (silica gel, 10 cm, ∅ = 4.5 cm, *n*-pentane/ethyl acetate, 7:3 v/v); yield 1.80 g (7.03 mmol, 91%). ^{1}H NMR ($CDCl_3$, 300 MHz, 25 °C): δ = 2.26 (s, 6 H, C^5-CH_3), 2.46 (s, 6 H, C^3-CH_3), 5.13 (dd, $^2J_{H,H}$ = 1.4 Hz, $^3J_{H,H}$ = 11.6 Hz, 2 H, (*Z*)-H_2C=), 5.28 (dd, $^2J_{H,H}$ = 1.4 Hz, $^3J_{H,H}$ = 17.9 Hz, 2 H, (*E*)-H_2C=), 6.08 (s, 2 H, -CH_2-), 6.46 (dd, $^3J_{H,H}$ = 17.9 Hz, $^3J_{H,H}$ = 11.6 Hz, 2 H, –HC=) ppm. ^{13}C NMR ($CDCl_3$, 75.5 MHz, 25 °C): δ = 10.2 (C^5-CH_3), 13.5 (C^3-CH_3), 60.7 (-CH_2-), 112.8 (=CH_2), 116.5 (C^4), 127.4 (–HC=), 138.0 (C^5), 146.8 (C^3) ppm. IR (KBr): $\tilde{\nu}$ = 1641 (s, C=C_{vinyl}), 1547 (m, C=N) cm^{-1}. FD-MS (CH_2Cl_2): *m*/*z* (%) = 257 (100) [MH^+]. $C_{15}H_{20}N_4$ (256.35 g mol^{-1}): calcd. C 70.28, H 7.86, N 21.86; found C 70.50, H 7.83, N 21.86.

Synthesis of Bis(3,5-dimethyl-4-vinylpyrazol-1-yl)acetic Acid (Hbdmvpza) (4): A solution of **3** (1.20 g, 4.68 mmol) in dry THF is treated with *n*-butyllithium (1.6 M solution in hexanes, 3.0 mL, 4.80 mmol) at –70 °C. The mixture is warmed to a temperature of –40 °C during a period of 4.5 h. A dry stream of CO_2 is bubbled through the mixture for 1 h and the resulting clear solution is slowly warmed to room temperature and stirred overnight. The solvent is removed under reduced pressure and the residue is dissolved in water (250 mL). The aqueous phase is washed with *n*-pentane (2 × 50 mL) to remove impurities. The remaining aqueous phase is acidified to pH = 2 with diluted HCl and extracted with ethyl ether (2 × 100 mL). The extract is dried with Na_2SO_4 and the solvent is removed under reduced pressure to yield a white powder of **4**; yield 1.20 g (4.00 mmol, 85%). ^{1}H NMR ($CDCl_3$, 300 MHz, 25 °C): δ = 2.23 (s, 6 H, C^5-CH_3), 2.31 (s, 6 H, C^3-CH_3), 5.21 (dd, $^2J_{H,H}$ =

0.8 Hz, $^3J_{H,H}$ = 11.6 Hz, 2 H, (*Z*)-H_2C=), 5.31 (dd, $^2J_{H,H}$ = 0.8 Hz, $^3J_{H,H}$ = 17.9 Hz, 2 H, (*E*)-H_2C=), 6.46 (dd, $^3J_{H,H}$ = 17.9 Hz, $^3J_{H,H}$ = 11.6 Hz, 2 H, –HC=), 6.91 (s, 1 H, –CH–) ppm. ^{13}C NMR ($CDCl_3$, 75.5 MHz, 25 °C): δ = 10.0 (C^5-CH_3), 13.3 (C^3-CH_3), 70.9 (-CH_2-), 114.5 (=CH_2), 117.6 (C^4), 126.6 (–HC=), 138.9 (C^5), 147.3 (C^3), 165.1 (CO_2H)ppm. IR (KBr): $\tilde{\nu}$ = 1734 (s, CO_2H), 1636 (s, C=C_{vinyl}), 1560 (w, C=N) cm^{-1}. FD-MS (CH_2Cl_2): *m*/*z* (%) = 256 (100) [$MH^+ - CO_2$], 301 (80) [MH^+]. $C_{16}H_{20}N_4O_2$ (300.36 g mol^{-1}): calcd. C 63.98, H 6.71, N 18.65; found C 64.22, H 6.70, N 18.93.

Synthesis of [Mn(bdmvpza)(CO)$_3$] (5): Hbdmvpza (**4**) (350 mg, 1.17 mmol) in dry THF (30 mL) is deprotonated with KO*t*Bu (131 mg, 1.17 mmol) for 1 h at ambient temperature. [$MnBr(CO)_5$] (320 mg, 1.17 mmol) is added and the reaction mixture is heated under reflux and controlled by IR spectroscopy on a regular basis. After completion of the reaction (approx. 17 h), the solvent is removed under reduced pressure. The yellow residue is washed with degassed water (5 × 10 mL) and diethyl ether (5 × 10 mL) and dried in vacuo to yield complex **5** as a yellow crystal powder. Crystals suitable for X-ray analysis can be obtained by layering a CH_2Cl_2 solution of **5** with diethyl ether. Yield 270 mg (0.616 mmol, 53%). ^{1}H NMR ($CDCl_3$, 300 MHz, 25 °C): δ = 2.44 (s, 6 H, C^5-CH_3), 2.61 (s, 6 H, C^3-CH_3), 5.38 (br., AMX system, coupling not resolved, 4 H, H_2C=), 6.45 (br., AMX system, coupling not resolved, 3 H, –HC = and –CH–) ppm. ^{13}C NMR ($CDCl_3$, 75.5 MHz, 25 °C): δ = 10.1 (C^5-CH_3), 13.9 (C^3-CH_3), 66.8 (–CH–), 117.8 (=CH_2), 118.6 (C^4), 125.5 (–HC=), 138.7 (C^5), 152.5 (C^3), 165.5 (CO_2^-), 219.9 (C=O), 223.1 (C=O) ppm. IR (THF): $\tilde{\nu}$ = 2036 (s, C=O), 1944 (s, C=O), 1917 (s, C=O), 1682 (m, CO_2^-), 1667 (m, C=C_{vinyl}) cm^{-1}. FAB-MS: *m*/*z* (%) = 439 (50) [MH^+], 383 (15) [$MH^+ - 2\times CO$], 355 [$MH^+ - 3\times CO$], 310 (100) [$MH^+ - 3\times CO - CO_2$]. $C_{19}H_{19}MnN_4O_5$ (438.32 g mol^{-1}): calcd. C 52.06, H 4.37, N 12.78; found C 52.17, H 4.46, N 12.58.

Synthesis of [Re(bdmvpza)(CO)$_3$] (6): Hbdmvpza (**4**) (350 mg, 1.17 mmol) in dry THF (30 mL) is deprotonated with KO*t*Bu (131 mg, 1.17 mmol) for 1 h at ambient temperature. [$ReBr(CO)_5$] (473 mg, 1.17 mmol) is added and the reaction mixture is heated under reflux and controlled by IR spectroscopy on a regular basis. After completion of the reaction (approx. 24 h), the solvent is removed under reduced pressure. The white residue is washed with degassed water (5 × 10 mL) and diethyl ether (5 × 10 mL) and dried in vacuo to yield complex **6** as a white crystal powder. Yield 270 mg (0.474 mmol, 41%). ^{1}H NMR ($CDCl_3$, 300 MHz, 25 °C): δ = 2.45 (s, 6 H, C^5-CH_3), 2.56 (s, 6 H, C^3-CH_3), 5.41 (br., AMX system, coupling not resolved, 4 H, H_2C=), 6.44 (dd, $^3J_{H,H}$ = 17.7 Hz, $^3J_{H,H}$ = 11.5 Hz, 2 H, –HC=), 6.63 (s, 1 H, –CH–) ppm. ^{13}C NMR ($CDCl_3$, 75.5 MHz, 25 °C): δ = 10.2 (C^5-CH_3), 14.7 (C^3-CH_3), 68.0 (–CH–), 118.5 (C^4), 118.7 (=CH_2), 125.1 (–HC=), 138.8 (C^5), 152.5 (C^3), 163.8 (CO_2^-), 194.9 (C=O), 196.0 (C=O) ppm. IR (THF): $\tilde{\nu}$ = 2026 (s, C=O), 1921 (s, C=O), 1898 (s, C=O), 1697 (m, CO_2^-) cm^{-1}. FD-MS (CH_2Cl_2): *m*/*z* (%) = 570 (100) [MH^+]. $C_{19}H_{19}N_4O_5Re$ (569.59 g mol^{-1}): calcd. C 40.06, H 3.36, N 9.84; found C 39.92, H 3.40, N 9.48.

Synthesis of [Ru(bdmvpza)Cl(PPh$_3$)$_2$] (7): A solution of Hbdmvpza (**4**) (450 mg, 1.50 mmol) in THF (25 mL) is deprotonated with KO*t*Bu (168 mg, 1.50 mmol) at ambient temperature. After one hour [$RuCl_2(PPh_3)_3$] (1.44 g, 1.50 mmol) is added and the mixture is stirred at ambient temperature for another 45 min. The solvent is removed in vacuo and the residue is washed with degassed water (3 × 20 mL) and diethyl ether (3 × 20 mL) and dried in vacuo to yield **7** as an orange crystal powder. Yield 960 mg (1.00 mmol, 67%). ^{1}H NMR ($CDCl_3$, 300 MHz, 25 °C): δ = 1.82 (s, 6 H, C^3-CH_3), 2.46 (s, 6 H, C^5-CH_3), 5.00 (dd, $^2J_{H,H}$ = 1.3 Hz, $^3J_{H,H}$ = 17.9 Hz, 2 H, (*E*)-H_2C=), 5.10 (dd, $^2J_{H,H}$ = 1.3 Hz $^3J_{H,H}$ = 11.7 Hz, 2 H, (*Z*)-H_2C=), 6.06 (dd, $^3J_{H,H}$ = 11.5 Hz, $^3J_{H,H}$ = 17.7 Hz, 2 H, –HC=), 6.64 (s, 1 H, –CH–), 6.95 (m, 12 H, PPh_3), 7.10 (m, 6 H, PPh_3), 7.41 (m, 12 H, PPh_3) ppm. ^{13}C NMR ($CDCl_3$, 75.5 MHz, 25 °C): δ =. 10.3 (C^5-CH_3), 15.2 (C^3-CH_3), 69.3 (CH), 115.8 (=CH_2), 119.0 (C^4), 126.2 (–HC=), 126.8 (vt, $J_{C,P}$ = 4.2 Hz, *m*-PPh_3), 128.3 (s, *p*-PPh_3), 134.8 (vt, $J_{C,P}$ = 4.2 Hz, *o*-PPh_3), 136.4 (t, $J_{C,P}$ = 39.3 Hz, *i*-PPh_3), 138.1 (C^5), 156.0 (C^3), 168.2 (CO_2^-) ppm. ^{31}P NMR ($CDCl_3$, 121.5 MHz, 25 °C): δ = 35.1 ppm. IR (KBr): $\tilde{\nu}$ = 1659 (s, CO_2^-), 1641 (m, C=C_{vinyl}) cm^{-1}. $C_{52}H_{49}ClN_4O_2P_2Ru$ (960.44 g mol^{-1}): calcd. C 65.03, H 5.14, N 5.83; found. C 64.89, H 5.09, N 5.71.

Synthesis of [Cu(bdmvpza)$_2$] (8): To a solution of Hbdmvpza (**4**) (300 mg, 1.00 mmol) in acetonitrile (15 mL) is added copper(II) acetate monohydrate (66.5 mg, 0.333 mmol). The reaction mixture is stirred for 6 h at ambient temperature. The turquoise precipitate is filtered off, washed with water (5 × 5 mL) and ethyl ether (5 × 5 mL) and dried in vacuo. Pale blue crystals suitable for an X-ray structure determination can be obtained by layering a CH_2Cl_2 solution of **8** with *n*-pentane; yield 135 mg (0.204 mmol, 61%). IR (KBr): $\tilde{\nu}$ = 1664 (s, CO_2^-), 1636 (m, C=C_{vinyl}), 1560 (w, C=N) cm^{-1}. UV (MeOH): λ_{max} = 690 nm. FD-MS (CH_2Cl_2): *m*/*z* (%) = 663 (10) [MH^+], 617 (10) [$MH^+ - CO_2$], 257 (100) [$C_{16}H_{20}N_4O_2 - CO_2$]. $C_{32}H_{38}CuN_8O_4$ (662.24 g mol^{-1}): calcd: C 58.04, H 5.78, N 16.92; found C 57.95, H 5.78, N 16.99.

General Procedure for the Copolymerisation of 3 or 4: To a solution of the co-monomer in dry xylene (10 mL) ligand **4** or ligand **3** is added and the solution is heated to 80 °C. After addition of azobisisobutyronitile (AIBN) the mixture is stirred under a nitrogen atmosphere. The polymer which precipitates during the reaction is separated by centrifugation and ground in a mortar. It is then added to a mixture of MeOH (300 mL and diluted HCl (3 mL), washed exhaustively with dry MeOH and finally dried in vacuo. The amount of copolymerised ligand is determined by elemental analysis. The yields of the polymers are given as weight percent related to the total weight of all monomer units.

P1a: Following the general procedure using Hbdmvpza (**4**) (100 mg, 0.332 mmol), destabilised methyl methacrylate (1.08 mL, 1.00 g, 9.99 mmol) and AIBN (20.0 mg, 120 μmol). Reaction time: 3.5 h; yield 338 mg (31%). Incorporation: 0.746 mmol g^{-1}.

P1b: The remaining xylene solution of experiment **P1a** is slowly poured into a mixture of MeOH (100 mL) and diluted HCl (1 mL) whereupon **P1b** starts to precipitate. The polymer is washed exhaustively with MeOH and dried in vacuo; yield 130 mg (12%). Incorporation: 0.304 mmol g^{-1}.

P2: Following the general procedure using Hbdmvpza (**4**) (100 mg, 0.332 mmol), destabilised ethylene glycol dimethacrylate (950 mL, 1.00 g, 5.04 mmol) and AIBN (20.0 mg, 120 μmol). Reaction time: 2.5 h; yield 850 mg (77%). Incorporation: 0.371 mmol g^{-1}.

Homopolymerisation of 4 (H1): Following the general procedure using Hbdmvpza (**4**) (300 mg, 1.00 mmol) as only monomer and AIBN (33.0 mg, 200 μmol). Reaction time: 3.5 h; yield 213 mg (71%). Incorporation: 3.05 mmol g^{-1}.

P3: Following the general procedure using destabilised methyl methacrylate (1.08 mL, 1.00 g, 9.99 mmol) and ligand **3** (100 mg, 0.332 mmol). After a reaction time of 4 h, the resulting polymer solution in xylene is slowly poured into a mixture of MeOH (300 mL) and diluted HCl (3 mL) whereupon **P3** precipitates. The polymer is washed exhaustively with MeOH and dried in vacuo; yield 744 mg (68%). Incorporation: 0.520 mmol g^{-1}.

Immobilisation of Mn on P1a (P1a-Mn): To a suspension of the copolymer **P1a** (100 mg, loading 0.746 mmol g^{-1}, 1.00 equiv.) in dry methanol (15 mL) is added KO*t*Bu (8.37 mg, 74.6 μmol) and the mixture is stirred at 50 °C under a nitrogen atmosphere. After 1.5 h [$MnBr(CO)_5$] (20.5 mg, 74.6 μmol) is added and the mixture was stirred for additional 24 h at 50 °C. The polymer is filtered of and washed with methanol and water and dried in vacuo to yield **P1a-Mn** as pale yellow powder. The content of manganese in the polymer is determined by AAS to 0.470 mmol g^{-1}. IR (nujol): $\tilde{\nu}$ = 2038 (CO), 1947 (CO), 1918 (CO).

Immobilisation of Re on P1a (P1a-Re): Following the procedure for **P1a-Mn**, using copolymer **P1a** (100 mg, loading 0.746 mmol g^{-1}, 1.00 equiv.), KO*t*Bu (8.37 mg, 74.6 μmol) and [$ReBr(CO)_5$] (30.3 mg, 74.6 μmol). The content of rhenium in the polymer is determined by ICP-AES to 0.311 mmol g^{-1}. IR (nujol): $\tilde{\nu}$ = 2028 (CO), 1923 (CO), 1898 (CO).

Immobilisation of Mn on P2 (P2-Mn): Following the procedure for **P1a-Mn**, using copolymer **P2** (150 mg, loading 0.371 mmol g^{-1}, 1.00 equiv.), KO*t*Bu (6.24 mg, 55.7 μmol) and [$MnBr(CO)_5$] (15.3 mg, 55.7 μmol). The content of manganese in the polymer is determined by AAS to 0.148 mmol g^{-1}. IR (nujol): $\tilde{\nu}$ = 2041 (CO), 1949 (CO), 1924 (CO).

Immobilisation of Re on P2 (P2-Re): Following the procedure for **P1a-Mn**, using copolymer **P2** (150 mg, loading 0.371 mmol g^{-1}, 1.00 equiv.), KO*t*Bu (6.24 mg, 55.7 μmol) and [$ReBr(CO)_5$] (22.6 mg, 55.7 μmol). The content of manganese in the polymer is determined by ICP-AES to 0.038 mmol g^{-1}. IR (nujol): $\tilde{\nu}$ = 2031 (CO), 1927 (CO), 1908 (CO).

Immobilisation of Cu on P1a (P1a-Cu): To a suspension of **P1a** (100 mg, loading 0.746 mmol g^{-1}, 1.00 equiv.) in dry methanol (10 mL) KO*t*Bu (8.37 mg, 74.6 μmol) is added and the suspension is stirred for 1 h at 50 °C under a nitrogen atmosphere. A solution of $CuCl_2$ (15 mg, 111 μmol) in methanol is added whereupon the residue immediately turns lime green. The polymer is filtered off, washed exhaustively with dry methanol and dried in vacuo to yield **P1a-Cu** as a lime green powder. UV (polymer film): λ_{max} = 754 nm.

Immobilisation of Fe on P1a (P1a-Fe): To a suspension of **P1a** (200 mg, loading 0.746 mmol g^{-1}, 1.00 equiv.) in dry methanol (10 mL) KO*t*Bu (16.4 mg, 0.150 mmol) is added and the suspension is stirred for 1 h at 50 °C under a nitrogen atmosphere. $FeCl_2$ (30.4 mg, 0.240 mmol is added and the mixture is stirred for 1 h at 50 °C. The polymer is filtered off, washed exhaustively with degassed methanol and dried in vacuo to yield **P1a-Fe** as a pale green powder. The content of iron was determined by AAS to 0.491 mmol g^{-1}. In a parallel experiment $FeSO_4$ was used as iron(II) source. In this case the iron content was determined to 0.448 mmol g^{-1}.

Immobilisation of Fe on P2 (P2-Fe): To a suspension of **P2** (1.00 g, loading 0.371 mmol g^{-1}, 1.00 equiv.) in dry methanol (10 mL) KO*t*Bu (41.6 mg, 0.371 mmol) is added and the suspension is stirred for 1 h at 50 °C under a nitrogen atmosphere. A solution of $FeCl_2$ (47.0 mg, 0.371 mmol) in methanol is added and stirred for 1 h at 50 °C. The polymer is filtered off, washed exhaustively with degassed methanol and dried in vacuo to yield **P2-Fe** as a pale green powder. The content of iron is determined by AAS to 0.165 mmol g^{-1}.

Synthesis of [Ru(bdmvpza)(BF)(PPh_3)] (9): To a solution of [Ru(bdmvpza)Cl(PPh_3)$_2$] (**7**) (462 mg, 0.481 mmol) in CH_2Cl_2 is added thallous acetate (152 mg, 0.577 mmol) and benzoylformic acid (90.3 mg, 0.601 mmol). The mixture is stirred 2 h at ambient temperature and then filtered through celite. The solvent is removed in vacuo. Precipitation from a CH_2Cl_2 solution with *n*-pentane yields **9** as deep purple powder. Yield 290 mg (0.357 mmol, 74%). ^{1}H NMR ($CDCl_3$, 300 MHz, 25 °C): δ = 1.91 (s, 3 H, C^{3a}-CH_3), 1.92 (s, 3 H, C^{3b}-CH_3), 2.50 (s, 3 H, C^{5b}-CH_3), 2.53 (s, 3 H, C^{5a}-CH_3), 5.05 (dd, $^2J_{H,H}$ = 1.0 Hz, $^3J_{H,H}$ = 17.9 Hz, 1 H, (*E*)-H_2C=), 5.20 (dd, $^2J_{H,H}$ = 1.1 Hz, $^3J_{H,H}$ = 11.5 Hz, 1 H, (*Z*)-H_2C=), 5.23 (dd, $^2J_{H,H}$ = 1.1 Hz, $^3J_{H,H}$ = 17.9 Hz, 1 H, (*E*)-H_2C=), 5.29 (dd, $^2J_{H,H}$ = 1.1 Hz, $^3J_{H,H}$ = 11.5 Hz, 1 H, (*Z*)-H_2C=), 6.23 (dd, $^3J_{H,H}$ = 11.5 Hz, $^3J_{H,H}$ = 17.7 Hz, 1 H, –HC=), 6.37 (dd, $^3J_{H,H}$ = 11.5 Hz, $^3J_{H,H}$ = 17.7 Hz, 1 H, –HC=), 6.60 (s, 1 H, –CH–), 7.20 (t, 6 H, *m*-PPh_3), 7.26 (m, 3 H, *p*-PPh_3), 7.32 (m, 8 H, *o*-PPh_3 and *m*-Ph), 7.53 (t, 1 H, *p*-Ph), 8.35 (d, 2 H, *o*-Ph) ppm. ^{13}C NMR ($CDCl_3$, 75.5 MHz, 25 °C): δ = 10.3 (2×C^5), 11.7 (C^{3b}), 14.2 (C^{3a}), 68.9 (–CH–), 116.5, 117.4 (2× = CH_2), 119.4 (C^{4a}), 119.0 (C^{4b}), 125.5, 125.8 (2× –HC=), 128.0 (*m*-Ph), 128.2 (d, $^3J_{CP}$ = 9.6 Hz, *m*-PPh_3), 129.6 (*p*-PPh_3), 130.3 (*o*-Ph_3), 133.5 (*i*-Ph), 134.1 (d, $^2J_{CP}$ = 9.0 Hz, *o*-PPh_3), 134.4 (*p*-Ph), 138.4 (C^{5b}), 140.0 (C^{5a}), 153.1(C^{3b}), 157.2 (C^{3a}), 167.9 (CO_2^-), 169.6 (CO_2^-), 202.9 (C=O) ppm. ^{31}P NMR ($CDCl_3$, 121.5 MHz, 25 °C): δ = 57.8 ppm. IR (KBr): $\tilde{\nu}$ = 1653 s (CO_2^-) cm^{-1}. IR (CH_2Cl_2): $\tilde{\nu}$ = 1660 (s, CO_2^-), 1652 (vs, CO_2^-) cm^{-1}. UV/Vis (MeOH): λ_{max} (log ε) = 554.5 (4.77) nm. $C_{42}H_{39}N_4O_5PRu$ (811.83 g mol^{-1}) calcd. C 62.14, H 4.84, N 6.90; found C 61.95, H 5.16, N 6.75%.

Synthesis of [Ru(bdmvpza)(NOG)(PPh_3)] (10): To a solution of [Ru(bdmvpza)Cl(PPh_3)$_2$] (**7**) (228 mg, 0.250 mmol) in CH_2Cl_2 is added thallous acetate (73.0 mg, 0.275 mmol) and *N*-oxalylglycine (50.0 mg, 0.305 mmol). The mixture is stirred 24 h at ambient temperature. The solvent was removed in vacuo, the residue is washed with degassed water (3 × 10 mL) and diethyl ether (3 × 10 mL) and dried in vacuo to yield complex **5** as an orange crystal powder. Crystals suitable for an X-ray structure determination can be obtained by layering a DMF solution of **10** with diethyl ether; yield 155 mg (0.192 mmol, 77%). ^{1}H NMR ([D_6]DMSO, 300 MHz, 25 °C): δ = 1.70 (s, 3 H, C^{3b}-CH_3), 1.98 (s, 3 H, C^{3a}-CH_3), 2.43 (s, 3 H, C^5-CH_3), 2.48 (s, 3 H, C^5-CH_3), 3.49 (dd, J_{AB} = 16.9 Hz, $^3J_{H,H}$ = 5.9 Hz, 1 H, -CH_2-NH), 3.65 (ABX, J_{AB} = 16.9 Hz, $^3J_{H,H}$ = 5.9 Hz, 1 H, -CH_2–CO_2H), 4.97 (d, $^3J_{H,H}$ = 17.7 Hz, 1 H, (*E*)=CH_2), 5.06 (d, $^3J_{H,H}$ = 11.3 Hz, 1 H, (*Z*) = CH_2), 5.29 (m, 2 H, =CH_2), 6.24 (dd, $^3J_{H,H}$ = 17.6 Hz, $^3J_{H,H}$ = 11.6 Hz, 1 H, -CH=), 6.53 (m, 2 H, CH and -CH=), 7.04 (m, 6 H, *o*-PPh_3), 7.20 (m, 6 H, *m*-PPh_3), 7.31 (m, 6 H, *p*-PPh_3), 9.15 (m, 1 H, NH) ppm. ^{13}C NMR ([D_6]DMSO, 75.5 MHz, 25 °C): δ = 9.9 (C^{5a}-CH_3), 10.0 (C^{5b}-CH_3), 10.9 (C^{3a}-CH_3), 13.4 (C^{3b}-CH_3), 41.5 (-CH_2-NH), 68.4 (CH), 115.4, 116.8 (2× = CH_2), 117.7, 118.0 (2× C^4), 125.9, 126.2 (2× -CH=), 127.9 (d, $^3J_{CP}$ = 24 Hz, *m*-PPh_3), 129.3 (*p*-PPh_3), 133.1 (*o*-PPh_3), 139.6 (C^{5a}), 141.4 (C^{5b}), 151.7 (C^{3a}), 155.9 (C^{3b}), 166.3 (CO_2^-), 167.1 (CO_2^-), 167.9 (C=O), 169.3 (CO_2H) ppm. ^{31}P NMR ([D_6]-DMSO, 121.5 MHz, 25 °C): δ = 60.7 ppm. IR (KBr): $\tilde{\nu}$ = 1673 (s, CO_2^-), 1623 (vs, (CO_2^-), 1543 w (C=N) cm^{-1}. UV/Vis (DMF): λ_{max} (log ε) = 300.4 (4.88) nm. $C_{38}H_{38}N_5O_7PRu$ (808.78 g mol^{-1}) calcd. C 56.43, H 4.74, N 8.66; found C 56.69, H 4.91, N 8.26%.

Synthesis of [Ru(bdmpza)(NOG)(PPh_3)] (11): To a solution of [Ru(bdmpza)(O_2CCH_3)(PPh_3)][5,23] (303 mg, 0.452 mmol) in CH_2Cl_2 is added *N*-oxalylglycine (75.0 mg, 0.510 mmol). The mixture is stirred 5 h at ambient temperature. The resulting orange precipitate is filtered of and washed with CH_2Cl_2 (3 × 2 mL) and dried in vacuo to yield complex **11** as an orange crystal powder. Crystals suitable for an X-ray structure determination can be obtained from a methanol solution of **11**; yield 256 mg (0.338 mmol, 75%). ^{1}H NMR ([D_6]DMSO, 250 MHz, 25 °C): δ = 1.70 (s, 3 H, C^{3b}-CH_3), 2.00 (s, 3 H, C^{3a}-CH_3), 2.49 (s, 6 H, C^{5a}-CH_3 and C^{5b}-CH_3), 3.60 (ABX, 2 H, J_{AB} = 17.0, $^3J_{HH}$ = 5.9 Hz, CH_2), 5.93 (s,

1 H, H_{pz}), 6.24 (s, 1 H, H_{pz}), 6.48 (s, 1 H, CH), 7.00–7.40 (m, 15 H, PPh_3), 9.26 (t, 1 H, $^3J_{HH}$ = 5.9 Hz, NH). ^{13}C NMR ([D$_6$]DMSO, 100.5 MHz): δ = 11.2 (C^{5a}-CH_3), 11.7 (C^{5b}-CH_3), 13.0 (C^{3a}-CH_3), 14.0 (C^{3b}-CH_3), 41.9 (-CH_2-NH), 69.2 (CH), 109.1, 109.4 (2× C^4), 128.6 (d, $^3J_{CP}$ = 8.7 Hz, *m*-PPh_3), 130.0 (*p*-PPh_3), 134.0 (br., *o*-PPh_3), 142.4 (C^{5a}), 144.5 (C^{5b}), 153.9 (C^{3a}), 158.1 (C^{3b}), 162.9 (CO_2^-), 167.9 (CO_2^-), 168.5 (C=O), 170.0 (CO_2H) ppm. ^{31}P NMR ([D$_6$]DMSO, 161.8 MHz): δ = 59.2 ppm. IR (KBr): $\tilde{\nu}$ = 1749 w (CO_2H), 1669 s (CO_2^-), 1624 vs. (CO_2^-), 1565 w (C=N), 1483 w, 1461 vw, 1434 m cm^{-1}. UV/Vis (DMF): λ_{max} (log ε) = 274.0 (3.69), 311.0 (3.86) nm. FAB-MS: *m*/*z* (%) = 758 (100) [MH^+], 566 (12) [MH^+ – $O_2CC(O)NHCH_2COOH$ – CO_2]. $C_{34}H_{34}N_5O_7PRu$ (756.72 g mol^{-1}): calcd. C 53.97, H 4.53, N 9.25; no suitable elemental analysis of **11** was obtained so far.

Polymerisation of Complex 9 with EGDMA (P-9): To a solution of [Ru(bdmvpza)(BF)PPh_3] (**9**) (100 mg, 0.123 mmol) and EGDMA (2.32 mL, 12.3 mmol) in acetonitrile (2.46 mL) at 65 °C is added AIBN (45.0 mg, 0.271 mmol). The mixture is allowed to stir for 24 h at this temperature under a nitrogen atmosphere. The resulting purple polymer is ground in a mortar and washed with MeOH prior to drying; yield 2.31 g. UV (nujol): λ_{max} = 558.5 nm.

Polymerisation of Complex 10 with EGDMA (P-10): To a solution of [Ru(bdmvpza)(NOG)PPh_3] (**10**) (28.0 mg, 34.6 μmol) and EGDMA (655 μL, 3.46 mmol) in a mixture of DMF (1.4 mL) and acetonitrile (1.4 mL) at 65 °C is added AIBN (12.5 mg, 76.2 μmol). The reaction mixture is allowed to stir for 24 h at this temperature under a nitrogen atmosphere. The resulting pale orange polymer is ground in a mortar and washed once with DMF and several times with MeOH prior to drying; yield 705 mg. UV (nujol): λ_{max} = 311.0 nm.

X-ray Structure Determination: Single crystals of **5**, **7**, **10** and **11** were mounted with Paratone N or perfluorated oil on a glass fibre. A modified Siemens P4 diffractometer (in case of **11**) or a Bruker–Nonius Kappa-CCD diffractometer was used for data collection. The structures were solved by using direct methods and refined with full-matrix least-squares F^2 {Siemens SHELX-97}.[27] A weighting Scheme was applied in the last steps of the refinement with $w = 1/[\sigma^2(F_o^2) + (aP)^2 + bP]$ and $P = [2Fc^2 + \max(F_o^2,0)]/3$. Most hydrogen atoms were included in their calculated positions and refined in a riding model. In case of complex **5** the asymmetric unit contained two molecules of **5** of which one was slightly disordered. The molecular structure of **7** contains one disordered dichloromethane per three molecules of **7**. The molecular structure of **10** contains one ethyl ether and two dimethylformamide solvent molecules per asymmetric unit, Squeeze/Platon was applied to resolve another severely disordered ethyl ether solvent molecule.[28] Within the 265.5 Å^3 of void space accessible to solvent molecules at a special position (x = 0.5, y = 1, z = 1), a total of 17.4 electrons were calculated, compared to 21 electrons predicted for the presence of half a diethyl ether molecule per asymmetric unit. Three methanol solvent molecules have been included in the structure model of **11**. All further details and parameters of the measurements are summarised in Table 4. The structure pictures were prepared with the program Diamond 2.1e.[29]

CCDC-729242 (for **5**), -729243 (for **7**), -762178 (for **10**) and -232650 (for **11**) contain the supplementary crystallographic data

Table 4. Details for structure determination of **5**, **7**, **10** and **11**.

	5	**7**	**10**	**11**
Empirical formula	$C_{19}H_{19}MnN_4O_5$	3 ($C_{32}H_{38}CuN_8O_4$) × CH_2Cl_2	2 ($C_{38}H_{38}N_5O_7PRu$) × $C_4H_{10}O$ × 2 C_3H_7NO	$C_{34}H_{34}N_5O_7PRu$ × 3 CH_3OH
Formula mass	438.32	2071.02	1837.86	852.83
Crystal colour/habit	yellow prism	blue prism	orange plate	red block
Crystal system	triclinic	trigonal	triclinic	triclinic
Space group	$P\bar{1}$	*R*-3	$P\bar{1}$	$P\bar{1}$
a [Å]	7.8676(4)	27.424(3)	14.4765(9)	11.412(7)
b [Å]	16.1761(12)	27.424(3)	14.8036(7)	12.577(6)
c [Å]	16.8239(18)	10.916(1)	22.3225(18)	14.113(8)
α [°]	71.768(8)	90	97.328(7)	101.81(3)
β [°]	80.814(7)	90	101.141(6)	97.86(6)
γ [°]	89.444(6)	120	101.191(4)	95.93(5)
V [Å^3]	2005.7(3)	7110.0(13)	1946.1(18)	1946.1(18)
θ [°]	2.73–28.5	2.73–28.5	2.83–28.00	2.16–26.01
h	–10 to 10	–36 to 30	–19 to 19	0 to 14
k	–21 to 21	–36 to 36	–19 to 19	–15 to 15
l	–22 to 22	–14 to 14	–29 to 29	–17 to 17
F(000)	904	3249	1908	884
Z	4	3	2	2
μ(Mo-K_α) [mm^{-1}]	0.696	0.799	0.438	0.506
Crystal size [mm^3]	0.23 × 0.16 × 0.06	0.23 × 0.22 × 0.09	0.19 × 0.12 × 0.04	0.5 × 0.4 × 0.3
$D_{calcd.}$ [g cm^{-3}], *T* [K]	1.452, 200(2)	1.452, 150(2)	1.346, 150(2)	1.455, 188(2)
Reflections collected	59038	21267	152591	8020
Independent reflections	10164	4003	21870	7613
Observed reflections, $I > 2\sigma(I)$	6290	2828	15410	5626
Parameter	559	217	1102	487
Weight parameter *a*	0.0617	0.0607	0.0663	0.0533
Weight parameter *b*	0.7693	27.0636	0.8188	4.3517
R_1 (obsd.)	0.0509	0.0464	0.0509	0.0546
R_1 (overall)	0.1023	0.0802	0.086	0.0865
wR_2 (obsd.)	0.1176	0.1212	0.1182	0.1185
wR_2 (overall)	0.1376	0.1421	0.1294	0.1337
Difference peak/hole [e/Å^3]	–0.418/0.111	–0.481/0.974	0.726 /–0.621	1.279 /–0.700

for this paper. These data can be obtained free of charge from The Cambridge Crystallographic Data Centre via www.ccdc.cam.ac.uk/data_request/cif.

Acknowledgments

Generous financial support by the Deutsche Forschungsgemeinschaft (DFG) (SFB 583) is gratefully acknowledged. We thank Mr. J. Schmidt for AAS measurements.

[1] a) A. Otero, J. Fernández-Baeza, A. Antiñolo, J. Tejeda, A. Lara-Sánchez, *Dalton Trans.* **2004**, *10*, 1499–1510; b) M. Costas, M. P. Mehn, M. P. Jensen, L. Que Jr., *Chem. Rev.* **2004**, *104*, 939–986; c) G. Parkin, *Chem. Rev.* **2004**, *104*, 699–767; d) C. Pettinari, R. Pettinari, *Coord. Chem. Rev.* **2005**, *249*, 663–691; e) A. Otero, J. Fernández-Baeza, A. Lara-Sánchez, J. Tejeda, L. F. Sánchez-Barba, *Eur. J. Inorg. Chem.* **2008**, *34*, 5309–5326, and references therein.
[2] A. Beck, B. Weibert, N. Burzlaff, *Eur. J. Inorg. Chem.* **2001**, 521–527.
[3] N. Burzlaff, I. Hegelmann, B. Weibert, *J. Organomet. Chem.* **2001**, *626*, 16–23.
[4] I. Hegelmann, A. Beck, C. Eichhorn, B. Weibert, N. Burzlaff, *Eur. J. Inorg. Chem.* **2003**, 339–347.
[5] R. Müller, E. Hübner, N. Burzlaff, *Eur. J. Inorg. Chem.* **2004**, 2151–2159.
[6] B. Kozlevčar, P. Gamez, R. d. Gelder, W. L. Driessen, J. Reedijk, *Eur. J. Inorg. Chem.* **2003**, 47–50.
[7] E. Hübner, G. Türkoglu, M. Wolf, U. Zenneck, N. Burzlaff, *Eur. J. Inorg. Chem.* **2008**, 1226–1235.
[8] J. M. Elkins, K. S. Hewitson, L. A. McNeill, J. F. Seibel, I. Schlemminger, C. W. Pugh, P. J. Ratcliffe, C. J. Schofield, *J. Biol. Chem.* **2003**, *278*, 1802–1806.
[9] L. Alaerts, J. Wahlen, P. A. Jacobs, D. E. D. Vos, *Chem. Commun.* **2008**, 1727–1737.
[10] M. I. Burguete, J. M. Fraile, J. I. García, E. García-Verdugo, C. I. Herrerías, S. V. Luis, J. A. Mayoral, *J. Org. Chem.* **2001**, *66*, 8893–8901.
[11] B. M. L. Dioos, I. F. J. Vankelecom, P. A. Jacobs, *Adv. Synth. Catal.* **2006**, *348*, 1413–1446.
[12] M. Tada, Y. Iwasawa, *Chem. Commun.* **2006**, 2833–2844.
[13] K. Heinze, A. Fischer, *Eur. J. Inorg. Chem.* **2007**, 1020–1027.
[14] a) K. Severin, *Curr. Opin. Chem. Biol.* **2000**, *4*, 710–714; b) K. Polborn, K. Severin, *Chem. Commun.* **1999**, 2481–2482; c) K. Polborn, K. Severin, *Chem. Eur. J.* **2000**, *6*, 4604–4611; d) K. Polborn, K. Severin, *Eur. J. Inorg. Chem.* **2000**, 1687–1692; e) A. Schiller, R. Scopelliti, M. Benmelouka, K. Severin, *Inorg. Chem.* **2005**, *44*, 6482–6492; f) E. Burri, M. Öhm, C. Daguenet, K. Severin, *Chem. Eur. J.* **2005**, *11*, 5055–5061; g) A. Schiller, R. Scopelliti, K. Severin, *Dalton Trans.* **2006**, 3858–3867.
[15] P. C. Kunz, N. E. Brückmann, B. Spingler, *Eur. J. Inorg. Chem.* **2007**, *3*, 394–399.
[16] E. Hübner, T. Haas, N. Burzlaff, *Eur. J. Inorg. Chem.* **2006**, 4989–4997.
[17] G. Türkoglu, S. Tampier, N. Burzlaff, manuscript in preparation.
[18] S. Julià, P. Sala, J. Del Marzo, M. Sancho, *J. Heterocycl. Chem.* **1982**, *19*, 1141–1145.
[19] A. S. Potapov, A. I. Khlebnikov, V. D. Ogorodnikov, *Russ. J. Org. Chem.* **2006**, *42*, 550–554.
[20] H. Friebolin, *Basic one- and two-dimensional NMR spectroscopy*, 4th ed., Wiley-VCH, Weinheim, **2005**.
[21] A. López-Hernández, R. Müller, H. Kopf, N. Burzlaff, *Eur. J. Inorg. Chem.* **2002**, 671–677.
[22] A. K. Ho, I. Iin, P. A. Gurr, M. F. Mills, G. G. Qiao, *Polymer* **2005**, *46*, 6727–6735.
[23] S. Tampier, R. Müller, A. Thorn, E. Hübner, N. Burzlaff, *Inorg. Chem.* **2008**, *47*, 9624–9641.
[24] W. Abel, G. Wilkinson, *J. Chem. Soc.* **1959**, 1501–1505.
[25] P. S. Hallmann, T. A. Stephenson, G. Wilkinson, *Inorg. Synth.* **1970**, *12*, 237–240.
[26] C. J. Cunliffe, T. J. Franklin, N. J. Hales, G. B. Hill, *J. Med. Chem.* **1992**, *35*, 2652–2658.
[27] G. M. Sheldrick, *Acta Crystallogr., Sect. A* **2008**, *64*, 112–122.
[28] a) P. Van der Sluis, A. L. Spek, *Acta Crystallogr., Sect. A* **1990**, *46*, 194–201; b) A. L. Spek, *J. Appl. Cryst.* **2003**, *36*, 7–13.
[29] K. Brandenburg, M. Berndt, *Diamond – Visual Crystal Structure Information System*, Crystal Impact GbR, Bonn (Germany), **1999**; For Software Review see: W. T. Pennington, *J. Appl. Crystallogr.* **1999**, *32*, 1028–1029.

Received: February 1, 2010
Published Online: May 14, 2010

